## Supplementary Methods

### Virus construction.

PRV151 and PRV152 were described elsewhere (Demmin *et al.*, 2001; Smith *et al.*, 2000). All remaining recombinant viruses were derived from the pBecker3 infectious clone (Smith & Enquist, 1999). PRV-GS4284 and PRV-GS4379 (referred to throughout this report as 'pUL25/R*' and 'pUL25/G', respectively) are both fluorescent viruses that express pUL25 fused to either mCherry (pUL25/R*) or GFP (pUL25/G). The FP was fused in-frame between aa 42 and 43 of pUL25 based on homology to a pUL25–GFP double in-frame fusion developed for HSV-1 (Cockrell *et al.*, 2009). Both pUL25–FP infectious clones were made by a two-step recombination process (Tischer *et al.*, 2006). The PCR primers used for this protocol were 5′-CTGGGCCCGCCCGGGCTTCAGCGAGGGCCTCGACGCGCGCGTGAGCAAGGGCGAGGAG-3′ and 5′-CGGCCGCGCGGCGGCGCGCGTTCGCGTGCGCCAGCGCGAGCTTGTACAGCTCGTCCATGC-3′. The primers provided homology to UL25 flanking the insertion site between codons 42 and 43. The underlined region of the primers provides homology to the pEP–GFP-in and pEP–mCherry-in template plasmids (Antinone & Smith, 2010; Tischer *et al.*, 2006).

PRV-GS2275 and PRV-GS4465 (referred to throughout this report as 'pUL36-G' and 'pUL36-R*') are viruses that express pUL36 with GFP or mCherry fused to the C terminus, respectively. As above, two-step recombination was completed using primers 5′-CTTCAACGTGGACCTATTTCAGGTCCGCCTGATTCTCGGTGTGAGCAAGGGCGAGGAGC-3′ and 5′-ACCGCAGAGGCAAACAAGTTGGGTAATAAACAATTTATTACTTGTACAGCTCGTCCATGCCG-3′ to create pUL36-G, where primers share homology to the C terminus and downstream non-coding sequence of the UL36 gene and the underlined portions have homology to template EP–GFP-in. pUL36-R* was made using identical primers to those above but with the 3′ nucleotide (C) in the first primer removed to allow amplification from the pEP–mCherry-in template.

Strain GS2484, referred to as 'CMV-G' throughout this manuscript, expressed soluble GFP driven by a cytomegalovirus (CMV) immediate-early promoter. The CMV-G infectious clone was created by releasing a cassette from template plasmid GS2435, 'pEP-CMV >GFP-in' that encodes CMV >GFP >poly(A) flanked by two large regions of homology to US4 (Antinone *et al.*, 2010). Simultaneous digestion with restriction enzymes *Pvu*II and *Afl*III released the cassette, which was recombined with pBecker3 using two-step recombination.

**Cells and viral propagation.**

Infectious clones derived from pBecker3 were transfected into PK15 as described previously (Luxton *et al.*, 2005). The resultant stock of virus was passaged once more to create a working stock. Titres of working stocks were obtained by performing plaque assays on PK15 cells as described previously (Smith & Enquist, 1999). Virus PRV-GS443L, termed 'G-pUL35' throughout this report, was plaque purified by isolating virus from a single large plaque from a heterogeneous mixture of plaque sizes. This heterogeneity was not observed in plaques from other viruses. Vero cells (used for imaging and plaque diameter assay) and PK15 cells were maintained in Dulbecco's modified Eagle medium (DMEM) supplemented with 10% bovine growth serum (BGS).

**Characterization of viral growth kinetics.**

Cell-associated virus and supernatants for single-step growth curves were harvested from PK15 cells at 2, 5, 8, 12 and 24 h post removal of inoculum and processed as described previously (Tirabassi & Enquist, 1998). Titres of all time points were quantified by plaque assay on PK15 cells.

Plaque sizes of viruses were measured using a viable-stain assay in Vero cells. Vero cells in six-well trays were infected with virus at a concentration of 60–250 p.f.u. per well. Cells were overlaid with 3 ml methocel media (DMEM supplemented with 2% BGS and 10 mg methyl cellulose $ml^{-1}$) and plaques were allowed to grow for 3 days. Monolayers were then stained by gently overlaying neutral red solution (cat# N6264; Sigma-Aldrich) diluted 1:10 in methocel media on top of the 3 ml methocel media already in the wells. After an overnight incubation, methocel medium was rinsed from cells with PBS. Six-well plates were scanned on an Epson Perfection V500 Photo scanner at a resolution of 2000 dpi and diameters were measured in pixels across the widest horizontal clearing.

**Infection of CD-1 mice.**

Male CD-1 mice (6 weeks old; Charles River) were maintained for at least 2 weeks under a 12:12 LD cycle, two to three mice per cage with food and water available *ad libitum*. Intranasal application of PRV was administered to animals anaesthetized by isofluorane (2.5–5.0%) inhalation. Viral stocks were maintained frozen at −80 °C and used immediately after being thawed. Each animal received 5 µl PRV ($8–9\times10^5$ p.f.u.) in each nostril. Behaviour was continuously video monitored and images were captured every 10 min. Time to death after inoculation was determined from recorded images and rounded to the nearest hour. *P*-values were determined by performing one-way ANOVA followed by a post-hoc Tukey–Kramer test.

Infections of CD-1 mice with PRV-WT in the ranges of $4.4\times10^4$–$4.4\times10^6$ p.f.u. per nostril showed no differences in mean time to death (data not shown). Based on these results, mice were infected with $8\times10^5$ p.f.u. per nostril.

**Microscopy of individual extracellular viral particles.**

Characterization of extracellular viral particle fluorescence was performed on virus purified from the supernatants of infected PK15 cells. Briefly, PK15 cells were infected with indicated strains of PRV at an m.o.i. of 5 and incubated for 18 h in phenol-red free DMEM/F12 media supplemented with 2% BGS. Supernatants were collected without disturbing adherent cells and cell debris was cleared by 10 min of centrifugation at 4800 ***g***. Cleared supernatant (8 ml) was underlaid with a 1 ml cushion of 10% Nycodenz in PBS in an SW41 centrifuge tube. Samples were centrifuged at 38500 ***g*** for 60 min. Media and the Nycodenz cushion were gently aspirated from pelleted virus, and the pellets were resuspended in 0.1 ml PBS and kept on ice for up to 3 h. Resuspended virus was diluted further 1:50 and 0.07 ml was pipetted into a chamber composed of a microscope slide and #1.5 thickness coverslip separated by pedestals of small coverslip shards. Chambers were sealed with VALAB (1:1:1 petroleum jelly, lanolin and beeswax) and imaged on a Nikon Eclipse TE2000 U wide-field fluorescence microscope with a Cascade II camera (Roper Scientific) and a 100×1.49 numerical aperture (NA) objective. GFP was imaged using a 470/40 nm excitation filter and 525/50 nm emission filter; mRFP1 and mCherry were both imaged using a 572/35 nm excitation filter and 632/60 nm emission filter. To determine particle brightness, multiple fields of particles were captured with exposure times of 2 s.

**Quantification of extracellular viral particle fluorescence.**

A custom algorithm for the MetaMorph software package (Molecular Devices) was used to quantify fluorescence intensity of individual extracellular virus particles. Briefly, the algorithm identifies multiple diffraction-limited fluorescent puncta that are consistent with individual virions (Smith *et al.*, 2001). Each spot is measured for total fluorescence intensity using a defined region of interest that is constant for all particles and experiments. To ensure that only fluorescence from a single diffraction-limited particle is included in a measurement, the algorithm excludes particles with significant overlap in emission projections. Automation of the algorithm allowed for quantification of hundreds of particles per sample.

**Fluorescence localization in Vero cells.**

Vero cells were infected with each indicated virus at an m.o.i. of 5. At indicated times p.i., Vero cells were imaged with a 60×1.40 NA objective on Nikon Eclipse TE2000-E wide-field fluorescence microscope and Photometrics CoolSnap HQ2 camera. All exposures shown are 200 ms, with the exception of Fig. 3(i) and Fig. 3(j). Images were scaled equivalently for PRV-UL25/R* and PRV-R-UL35 viruses, and equivalently for PRV-R-UL36 and PRV-UL36-R* viruses.

**Quantification of particle velocities in chick neurons.**

Primary dorsal root ganglia (DRG) were isolated from day E8 chick embryos and grown for 2 days on coverslips treated with polyornithine and laminin. DRG were infected with $3.5\times10^5$ p.f.u. of either PRV-UL25/R* or PRV-R-UL35 virus. Fifteen minutes p.i., coverslips were imaged for 30 min. Moving particles were detected by time-lapse fluorescence microscopy in the red fluorescence channel at 10 frames per second (100 ms exposures) in 30 s intervals. Particle velocities were determined using the kymograph function of the MetaMorph software package. Kymographs were generated using the 'Multi-line' tool with a width of 20 pixels and 'average background' subtraction. Entire particle paths, whether moving, stalled or reversing, were traced within the kymograph using the 'Multi-line' tool. Data were filtered post analysis to only include velocities of runs ≥1.0 μm. The movement of 100 particles was analysed for each fluorescent virus; 560 and 481 runs were quantified for PRV-R-UL35 or PRV-UL25/R*, respectively.

**References**

**Antinone, S. E. & Smith, G. A. (2010).** Retrograde axon transport of herpes simplex virus and pseudorabies virus: a live-cell comparative analysis. *J Virol* **84**, 1504–1512. doi:10.1128/JVI.02029-09 Medline

**Antinone, S. E., Zaichick, S. V. & Smith, G. A. (2010).** Resolving the assembly state of herpes simplex virus during axon transport by live-cell imaging. *J Virol* **84**, 13019–13030. doi:10.1128/JVI.01296-10 Medline

**Cockrell, S. K., Sanchez, M. E., Erazo, A. & Homa, F. L. (2009).** Role of the UL25 protein in herpes simplex virus DNA encapsidation. *J Virol* **83**, 47–57. doi:10.1128/JVI.01889-08 Medline

**Demmin, G. L., Clase, A. C., Randall, J. A., Enquist, L. W. & Banfield, B. W. (2001).** Insertions in the gG gene of pseudorabies virus reduce expression of the upstream Us3 protein and inhibit cell-to-cell spread of virus infection. *J Virol* **75**, 10856–10869. doi:10.1128/JVI.75.22.10856-10869.2001 Medline

**Luxton, G. W., Haverlock, S., Coller, K. E., Antinone, S. E., Pincetic, A. & Smith, G. A. (2005).** Targeting of herpesvirus capsid transport in axons is coupled to association with specific sets of tegument proteins. *Proc Natl Acad Sci U S A* **102**, 5832–5837. doi:10.1073/pnas.0500803102 Medline

**Smith, B. N., Banfield, B. W., Smeraski, C. A., Wilcox, C. L., Dudek, F. E., Enquist, L. W. & Pickard, G. E. (2000).** Pseudorabies virus expressing enhanced green fluorescent protein: A tool for in vitro electrophysiological analysis of transsynaptically labeled neurons in identified central nervous system circuits. *Proc Natl Acad Sci U S A* **97**, 9264–9269. doi:10.1073/pnas.97.16.9264 Medline

**Bohannon, K. P., Sollars, P. J., Pickard, G. E. and Smith, G. A. (2012).** Fusion of a fluorescent protein to the pUL25 minor capsid protein of pseudorabies virus allows live-cell capsid imaging with negligible impact on infection. *J Gen Virol* **93**, 124–129.

**Smith, G. A. & Enquist, L. W. (1999).** Construction and transposon mutagenesis in Escherichia coli of a full-length infectious clone of pseudorabies virus, an alphaherpesvirus. *J Virol* **73**, 6405–6414. Medline

**Smith, G. A., Gross, S. P. & Enquist, L. W. (2001).** Herpesviruses use bidirectional fast-axonal transport to spread in sensory neurons. *Proc Natl Acad Sci U S A* **98**, 3466–3470. doi:10.1073/pnas.061029798 Medline

**Tirabassi, R. S. & Enquist, L. W. (1998).** Role of envelope protein gE endocytosis in the pseudorabies virus life cycle. *J Virol* **72**, 4571–4579. Medline

**Tischer, B. K., von Einem, J., Kaufer, B. & Osterrieder, N. (2006).** Two-Step Red-Mediated Recombination for Versatile High-Efficiency Markerless DNA Manipulation in *Escherichia coli*, pp. 191–197. United States: Biotechniques.

**Supplementary Table S1.** All viruses used in this study are summarized

| Strain | Name | Isogenic with | Titre (p.f.u. $ml^{-1}$) | Fluorophore | Position |
|---|---|---|---|---|---|
| PRV-GS999 | WT | PRV-Becker | $7.8\times10^8$ | None | NA |
| PRV-GS847 | R-pUL35 | PRV-Becker | $8.7\times10^8$ | mRFP1 | N terminus |
| PRV-GS443L | G-pUL35 | PRV-Becker | $5.7\times10^8$ | eGFP | N terminus |
| PRV-GS4284 | pUL25/R* | PRV-Becker | $2.0\times10^9$ | mCherry | aa 42–43† |
| PRV-GS4379 | pUL25/G | PRV-Becker | $7.0\times10^8$ | eGFP | aa 42–43† |
| PRV-GS962 | R-pUL36 | PRV-Becker | $6.3\times10^8$ | mRFP1 | N terminus |
| PRV-GS935 | G-pUL36 | PRV-Becker | $1.9\times10^9$ | eGFP | N terminus |
| PRV-GS2275 | pUL36-G | PRV-Becker | $5.4\times10^8$ | eGFP | C terminus |
| PRV-GS4465 | pUL36-R* | PRV-Becker | $1.1\times10^9$ | mCherry | C terminus |
| PRV-GS2484 | CMV-G | PRV-Becker | $2.4\times10^8$ | eGFP | US4 (disrupted)‡ |
| PRV151 | PRV151 (CMV-G) | PRV-Becker | $4.3\times10^8$ | eGFP | US4 (disrupted)‡ |
| PRV152 | PRV152 (CMV-G) | PRV-Bartha | $1.3\times10^9$ | eGFP | US4 (disrupted)‡ |

†Fluorophore fused to pUL25 as a double in-frame fusion between codons 42 and 43.

‡CMV >GFP >poly(A) cassette inserted into the gene US4, disrupting the coding sequence.

**Bohannon, K. P., Sollars, P. J., Pickard, G. E. and Smith, G. A. (2012).** Fusion of a fluorescent protein to the pUL25 minor capsid protein of pseudorabies virus allows live-cell capsid imaging with negligible impact on infection. *J Gen Virol* **93**, 124–129.

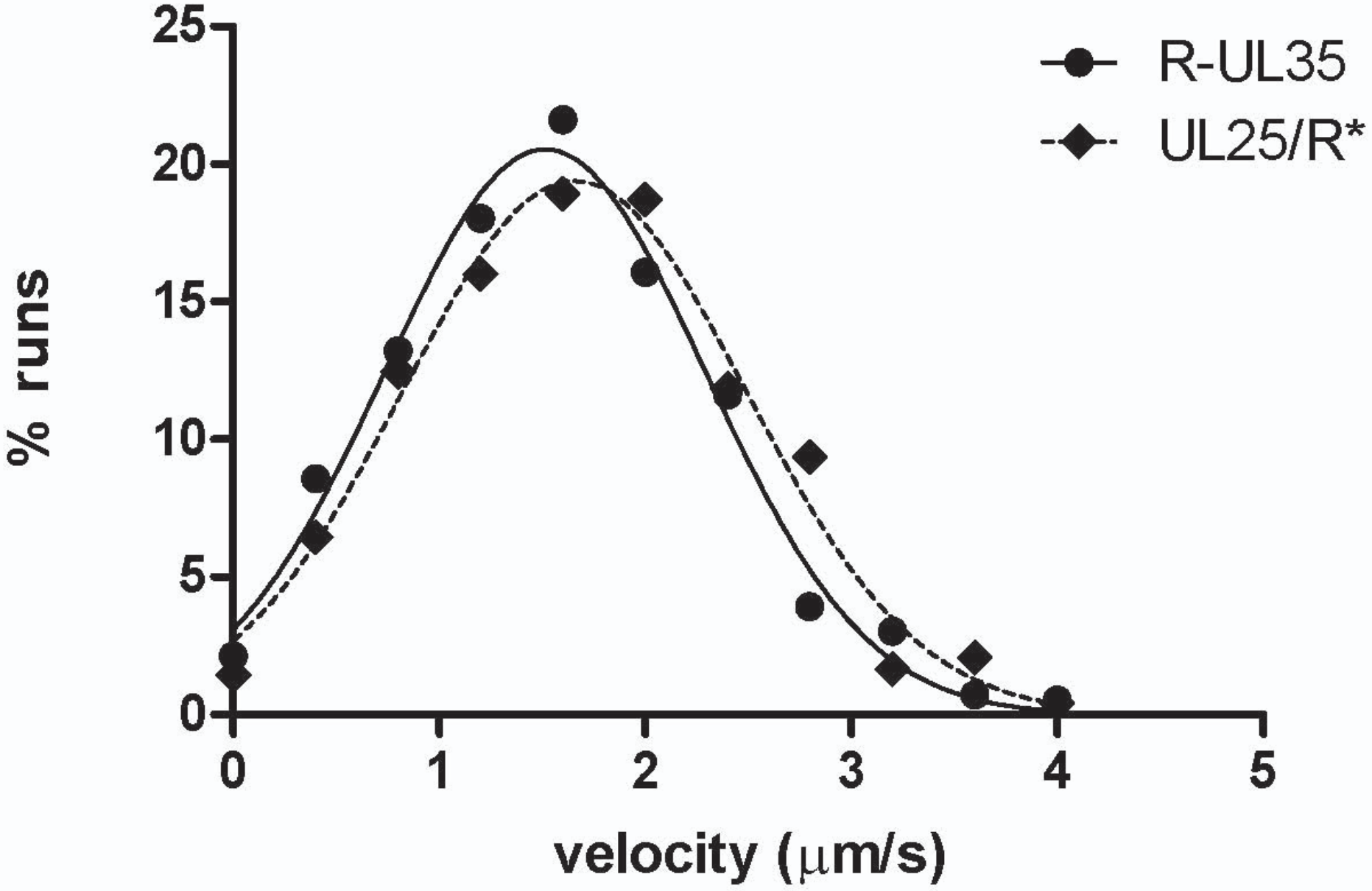
25
20
15
10
5
0
% runs
0
1
2
3
4
5
velocity (μm/s)
R-UL35
UL25/R*

**Supplementary Fig. S1.** Velocities of moving capsids in chick DRG. All velocities were obtained from capsids runs with length ≥1um. Bin size=0.4 μm $s^{-1}$. Gaussian non-linear regression was used to fit each dataset with $R^2$ >0.97. Additional non-linear regression analysis revealed that a single Gaussian curve could fit both curves with an $R^2$ >0.96, indicating the velocity profiles of the two viruses were indistinguishable (not shown).

**Bohannon, K. P., Sollars, P. J., Pickard, G. E. and Smith, G. A. (2012).** Fusion of a fluorescent protein to the pUL25 minor capsid protein of pseudorabies virus allows live-cell capsid imaging with negligible impact on infection. *J Gen Virol* **93**, 124–129.